Multiterminal molecular wire systems: A self-consistent theory and computer simulations of charging and transport

Eldon G. Emberly and George Kirczenow
Department of Physics, Simon Fraser University, Burnaby, British Columbia, Canada V5A 1S6
(Received 4 May 2000)

We present a self-consistent method for the evaluation of the electronic current flowing through a multiterminal molecular wire. The method is based on Büttiker-Landauer theory, which relates the current to one-electron scattering probabilities. The scattering problem is solved using a tight-binding form for Schrödinger's equation that incorporates a self-consistent evaluation of the electrostatic potential in the region of the molecular wire. We apply the method to a three-terminal molecular wire connected to metallic leads. The molecular wire is a π-conjugated carbon chain with thiol end groups, self-assembled on the cleaved edge of a multilayer of alternating thin metal and insulating films. The ends of the chain bond to two outer metal layers that act as source and drain, and the chain bridges a third (inner) metal layer that acts as a gate. We show that transistor action should occur in this device if on the surface of the metal gate there are adsorbed atoms that acquire charge as the gate voltage is increased, thereby enhancing the interaction between the gate and molecule and creating a strong potential barrier that hinders electron flow along the molecular wire. We find that electronic solitons play an important role in the response of this system to applied voltages.

I. INTRODUCTION

A molecular wire in its simplest definition is a single molecule that is used as a bridge to carry electronic current between metallic contacts. Recently developed techniques that allow manipulation of matter at the atomic scale have made remarkable experiments on molecular wires possible. Some of the first experiments measuring the current through single molecules employed the scanning tunneling microscope[1,2] (STM) or used self-assembly to bridge the gap between two nanoscopic metal leads with a single molecule (1,4 benzenedithiolate) whose current-voltage characteristic was then measured.[3] These and other two-terminal measurements[4–7] have shown that a molecular wire does not behave like a simple Ohmic resistor but displays features arising from the quantum states of the molecule. Theoretical work on molecular wires has proposed various models for the explanation of the observed phenomena and has until now focused on two-terminal devices.[8–12]

For two-terminal mesoscopic systems, Landauer theory[13] relates the electronic current to the transmission probability for a single electron to scatter through the system. Coherent transport in multiterminal mesoscopic systems has been treated by Büttiker, who has given an extension of Landauer theory,[14] and Christen and Büttiker have discussed charging effects in such systems.[15] However, to date there has been very little theoretical work done addressing these issues in the context of multiterminal molecular wire systems.[16]

In this paper, we present a self-consistent method based on Büttiker-Landauer theory for the evaluation of electronic current in a multiterminal molecular wire system. This method considers explicitly the effects of charging in molecular wires due to the application of voltages to the terminals. The theory is then applied to a molecular wire transistor (a three-terminal molecular wire device). The system we consider is a π-conjugated chain molecule with thiol end groups self-assembled onto the cleaved edge of a multilayer substrate. The substrate consists of alternating metal and insulating thin films. The chain bridges two of the metal films and passes over a third metal film which acts as a gate. For the system considered we find that transistorlike behavior is possible if the electric field of the gate is enhanced by chargeable adsorbates on its surface. We also find that charge density waves and charged solitons form in this molecular wire system and play an important role in its response to applied bias voltages.

Section II summarizes briefly the necessary results from Büttiker-Landauer theory for the evaluation of the electronic current in a multiterminal molecular wire. A method for solving the single-electron scattering problem is presented in Sec. III. Our self-consistent method for determining the electrostatic potential is presented in Sec. IV. These methods are then applied to the calculation of the charging behavior and current vs gate bias voltage characteristics of a three-terminal molecular wire transistor in Sec. V. Our conclusions are given in Sec. VI. An Appendix describing the electrostatics of the molecular wire configuration that was studied is also included.

II. MULTITERMINAL BÜTTIKER-LANDAUER THEORY

For two-terminal mesoscopic systems (such as a molecule bridging two metallic electrodes), the electronic current can be calculated using Landauer theory.[13] The systems that will be of interest in this article have more than two metallic contacts and thus it is necessary to have a method for calculating the current in these multiterminal structures. Büttiker and Christen have generalized Landauer theory to provide a theoretical framework for treating transport at finite voltages for systems connected to more than two leads.[14,15] We give a brief summary of their relevant results.

Consider a mesoscopic conductor (such as a molecular wire) attached to N different terminals or reservoirs

$\alpha=1,\ldots,N$. Each of these reservoirs may be at a different electrochemical potential μ_α. The important quantity is the difference between each of these electrochemical potentials and a common reference electrochemical potential μ_0, $\delta\mu_\alpha=\mu_\alpha-\mu_0$. This can be related to the bias voltage applied to the reservoir by $\delta\mu_\alpha=-eV_\alpha$. The current flowing into one of these reservoirs will be related to the probability for an electron to scatter into that reservoir; however, now there are more scattering processes that can occur. An electron scattering from the α' reservoir to the α reservoir is assigned a transmission probability $T_{\alpha,\alpha'}$. Reflection within the α reservoir is described by the reflection probability R_α. The net current flowing into the αth reservoir has several contributions. Electrons scatter into it from every other reservoir, and the current contributed by the α' reservoir is $\delta i_{\alpha,\alpha'}=-(2e/h)T_{\alpha,\alpha'}\delta\mu_{\alpha'}$. There is also a contribution due to reflected electrons and this is given by $\delta i_{\alpha,\alpha}=-(2e/h)R_\alpha\delta\mu_\alpha$. Adding these two contributions gives the total current flowing into reservoir α. However, there is also current flowing out of reservoir α and this is given by $-(2e/h)\delta\mu_\alpha$. The net current flowing into reservoir α is given by the difference between these contributions. Combining these terms, the current contribution in the lead connected to terminal α due to small differences in the electrochemical potentials is given by

$$\delta i_\alpha=-\frac{2e}{h}\left((1-R_\alpha)\delta\mu_\alpha-\sum_{\alpha'}T_{\alpha,\alpha'}\delta\mu_{\alpha'}\right). \tag{1}$$

This can be generalized to finite temperature T and finite voltages by integrating over the Fermi distributions, $F(E,V_\alpha)=1/\{\exp[-(E-\mu_\alpha)/kT]+1\}$ of each of the reservoirs. This gives

$$i_\alpha=-\frac{2e}{h}\int dE\left(1-R_\alpha(E,\{V_\gamma\})F(E,V_\alpha)-\sum_{\alpha'}T_{\alpha,\alpha'}(E,\{V_\gamma\})F(E,V_{\alpha'})\right). \tag{2}$$

This equation properly reduces to the two-terminal result if $T_{1,2}=T_{2,1}=T$ and $1-R_\alpha=T$.

The transmission and reflection probabilities that enter Eq. (2) depend on the electric fields throughout the system that arise from the application of the bias voltages and from the charges on the molecule. A later section provides a self-consistent method for handling this problem.

III. MULTITERMINAL SCATTERING THEORY

A variety of techniques exist for the evaluation of the relevant scattering probabilities that go into the calculation of the current. The method that we use determines these quantities directly from the single-electron wave function. The wave function is calculated by solving Schrödinger's equation for the scattered electron. Thus the problem is to find the wave function $|\Psi^\alpha\rangle$ for an electron with energy E incident from reservoir α. This wave function satisfies

$$[H-e\Phi(\{q\},\{V\})]|\Psi^\alpha\rangle=E|\Psi^\alpha\rangle, \tag{3}$$

where H is the single-electron Hamiltonian of the coupled system in the absence of applied biases and Φ is the electrostatic potential that depends upon the voltages $\{V\}$ applied to the terminals and the charges $\{q\}$ in the system. For simplicity, we assume that each of the reservoirs has only one electronic mode (the generalization to multichannel reservoirs is straightforward but the notation becomes complicated). We represent the system of leads and molecule using the tight-binding approximation with an orthogonal set of atomic orbitals. The molecule has a set of atomic orbitals $\{|\phi_j\rangle\}$. Each of the N reservoirs also has a set of orbitals and these are denoted $\{|n_\alpha\rangle\}$ where $n_\alpha=1,\ldots,\infty$ on the αth reservoir. The complete wave function can be written as a sum of the wave functions in each of the reservoirs α and the wave function on the molecule (M) $|\Psi^\alpha\rangle=\Sigma_{\alpha'}|\psi_{\alpha'}\rangle+|\psi_M\rangle$. The boundary conditions on these wave functions are the following for an electron incident from the αth reservoir:

$$|\psi_\alpha\rangle=\sum_{n=1}^{\infty}\exp(-iny^\alpha)|n_\alpha\rangle+r_\alpha\sum_{n=1}^{\infty}\exp(iny^\alpha)|n_\alpha\rangle, \tag{4a}$$

$$|\psi_{\alpha'}\rangle=t_{\alpha',\alpha}\sum_{n=1}^{\infty}\exp(iny^{\alpha'})|n_{\alpha'}\rangle, \tag{4b}$$

$$|\psi_M\rangle=\sum_j c_j^\alpha|\phi_j\rangle. \tag{4c}$$

Inserting the above wave function into Schrödinger's equation yields an infinite set of linear equations in the unknowns r_α, $t_{\alpha',\alpha}$, and c_j^α. Applying the bras $\langle 1_\alpha|$ where $\alpha=1,\ldots,N$ and $\{\langle\phi_j|\}$ yields a solvable set of linearly independent equations.

With the scattering coefficients determined the transmission and reflection probabilities for multiterminal scattering are found from

$$T_{\alpha',\alpha}\frac{v'_\alpha}{v_\alpha}|t_{\alpha',\alpha}|^2, \tag{5a}$$

$$R_\alpha=|r_\alpha|^2, \tag{5b}$$

where v_α is the velocity of an electron with energy E in the αth reservoir.

IV. NONEQUILIBRIUM CHARGE DISTRIBUTION AND THE SELF-CONSISTENT POTENTIAL

In this section the question of how to deal with the electric field due to the applied voltages and the charge in the system will be addressed.

The electrostatic potential energy $-e\Phi$ has several contributions. First, there is the contribution of the electrostatic potential due to the presence of the reservoirs, each at a different voltage bias. This is found from the solution to Laplace's equation $\nabla^2\phi(\vec{r},\{V_\alpha\})=0$ subject to the boundary condition that the surface of each reservoir is an equipotential. Secondly, the electrostatic field will induce a nonequilibrium charge distribution on the molecule. Because of this and because of chemical charge transfer effects between different atoms that occur even in the absence of bias voltages,

the atoms along the wire will no longer be electrically neutral, and this can be quantified as fractional ionization charge q_j for atom j on the molecule ($q_j<0$ corresponds to a negatively charged ion). At the mean-field level of approximation a propagating electron at position $\vec{r}$ will now interact with these charges via an unscreened Coulomb potential. And lastly these induced charges will in turn generate image charges in all of the metallic contacts. Thus the electrostatic energy terms that must be included in a mean-field treatment of the molecular wire are

$$-e\Phi=-e\phi(\vec{r},\{V_\alpha\})-e\sum_j \frac{q_j}{4\pi\epsilon_o}\frac{1}{|\vec{r}-\vec{r}_j|} -e\phi_{image}(\vec{r},\{q_j\}). \tag{6}$$

The potentials $\phi(\vec{r},\{V_\alpha\})$ and $\phi_{image}(\vec{r},\{q_j\})$ both depend on the system's geometry. A solution for the specific three-terminal geometry considered below is presented in the Appendix.

Within the tight-binding approximation, the presence of the electrostatic terms modifies the site energy of each orbital on the molecule. For instance, if each atom of the molecule has only a single orbital, then the diagonal element $H_{i,i}=\langle i|H-e\Phi|i\rangle$ for the ith atom of the molecule becomes

$$H_{i,i}=\epsilon_i(q_i)-e\phi(\vec{r}_i)-e\sum_{j\neq i}\frac{q_j}{4\pi\epsilon_o}\frac{1}{|\vec{r}_i-\vec{r}_j|} -e\phi_{image}(\vec{r}_i,\{q_j\}),$$

where $\epsilon_i(q_i)$ is a charge dependent site energy for atom i. In the chemistry literature $\epsilon_i(q_i)$ is usually taken to be a linear or quadratic fit to ionization potential energy data. Thus

$$\epsilon_i(q_i)=\epsilon_i^0+q_iU+(\text{term in } q^2),$$

where ϵ_i^0 is roughly equal to the average of the ionization energies for the positive ion and negatve ion (although the best fit may depart from this), and U is an energy associated with fractional charging.[17] This treatment of the on-site energies can also be regarded as a tight-binding version of the local density approximation, since the first-order variation of the charge density contribution to the site energy generates a linear term associated with the derivative of the site energy with respect to the fractional charge.

Thus the problem that now needs to be addressed is the determination of the charge on the wire. This is a self-consistent problem. The scattering problem must be solved to determine the charge. Then this charge must be used to adjust the effective Hamiltonian, and then the scattering problem must be solved again. This must be repeated until the charge on the wire converges.

In each iteration the charge is calculated as follows. Since the wave function is being calculated explicitly from Schrödinger's equation, the probability of an electron being on a certain site j on the molecule is given by $|c_j|^2$ for a given scattering state. The spectral charge on that site contributed by an electron incident with energy E (propagating in a Bloch state with wave vector k^α) from reservoir α is simply $-e|c_j^\alpha|^2$. Hence the charge on site j due to electrons incident from lead α is found by integrating over all the occupied Bloch states in that reservoir. The total charge is then found by summing over all the reservoirs. [Normalization has not been considered yet. The proper normalization for a scattering state $|\Psi^\alpha\rangle$ is $1/\sqrt{N}$ (where N is the number of unit cells) since this is the normalization for a propagating Bloch wave that will exist deep within the reservoirs. Thus, in the above, the charge needs to be divided by N.] Thus the charge can be written (including a factor of 2 for spin) as

$$q_j=-2e\sum_\alpha\sum_{k^\alpha}|\Psi_j^\alpha(k^\alpha)|^2=-\frac{2e}{N}\sum_\alpha\sum_{k^\alpha}|c_j^\alpha(k^\alpha)|^2.$$

Converting the wave vector sum into an integral (and making a change of variables to the reduced wave vector $y^\alpha=k^\alpha a$) results in

$$q_j=-\frac{2e}{N}\frac{L}{2\pi a}\sum_\alpha\int_0^{y_F}dy^\alpha|c_j^\alpha(y^\alpha)|^2.$$

Finally, converting the above wave vector integral into an energy integral over the energy band of each reservoir α, using $L=Na$, and generalizing to finite temperatures and voltages by using the Fermi function for reservoir α, $F(E,V_\alpha)$, the following expression is arrived at for the total charge on atom j of the molecule:

$$q_j=-\frac{2e}{2\pi}\sum_\alpha\int dE\frac{dy^\alpha}{dE}|c_j^\alpha(E)|^2F(E,V_\alpha). \tag{7}$$

In this article the atomic positions are assumed fixed; the effects of relaxing atoms in the calculation of the self-consistent potential will be discussed elsewhere. We now consider an application of the above method to a multiterminal molecular wire system.

V. MOLECULAR TRANSISTOR

In this section we present a feasible suggestion for a molecular wire transistor (MWT) and study it theoretically by the methods described above. A simple transistor functions by transmitting a current between an electron source and drain and tuning this current by the application of a voltage to a gate. At low gate voltages, current flows freely through the transistor under an applied bias between the source and drain. As the gate voltage increases an electrostatic barrier forms and the current decreases significantly. Whether behavior of this type can be exhibited by a single-molecule device (a MWT) has been a long-standing open question both experimentally and theoretically. The solid state transistor operates essentially on classical electromagnetic principles—an electric field suppresses the flow of electrons, which is governed by Boltzmann diffusion. When electrons flow through a molecule, their dynamics is governed not by classical physics but by quantum physics and the length and energy scales involved are also very different from those in solid state transistors. We show that these physical differences are very important, but that they can be addressed and that a working MWT should be feasible.

The greatest experimental challenge in developing a MWT is the introduction of the third terminal which should act as the gate. To date this has been achieved only in experiments on carbon nanotubes that were contacted lithographically to metal leads at the ends and then a gate potential was applied via a STM tip that was brought close to the

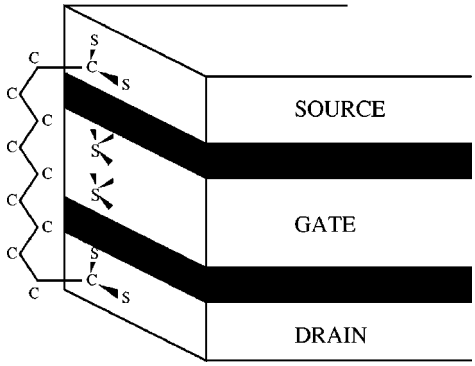

FIG. 1. Schematic of a molecular wire transistor. The substrate contains three gold layers that act as source, drain, and gate. The source is bridged to the drain by a π-conjugated carbon chain. Sulfur ions on the gate enhance the electrostatic coupling between the gate and carbon chain.

middle of the tube.[18,19] In the present work a three-terminal structure is considered, consisting of a molecule *self-assembled* on the cleaved edge of a multilayer consisting of three metallic films, each a few monolayers thick and separated from the other metal layers by thin insulating layers (as is shown schematically in Fig. 1). In the figure the outermost metal layers act as source and drain, and the inner layer is the gate. Although such structures have not yet been realized experimentally, it is reasonable to expect that they will be fabricated in the future. Our purpose here is to explore theoretically the fundamental principles that will help to guide experimental work on such systems.

The molecule that is considered is a π-conjugated carbon chain molecule terminated with thiol (sulfur) groups. The π conjugation provides for relatively easy electron transport along the chain between source and drain; such chains when strongly coupled to metallic leads are very conductive (relative to other molecular conductors). The thiols make for strong bonds between the ends of the chain and the source and drain, respectively, and are responsible for self-assembly of the MWT on the substrate. In the absence of the gate, this is just a two-terminal molecular device, broadly similar to the molecular wires that have already been discussed and studied experimentally.[1–3]

The conducting layers of the substrate are assumed to be gold. At the Fermi energy of gold, electrons on the molecular chain reside in orbitals that are π-like. Thus, when the chain is bonded between the source and drain, transport of electrons is along the conjugated π backbone of the chain. In the self-assembled structure shown in Fig. 1 the carbon chain is oriented such that these π orbitals are parallel to the substrate's surface; this implies a low probability of electron hopping between the surface and molecule.

In the tight-binding scheme, only the π orbital of each carbon atom is taken into account and it is assigned a site energy of -11.4 eV. The structure of the chain is taken to be undimerized trans-polyacetylene. Only nearest neighbor hopping is considered on the chain and a value of -2.5 eV is assigned to the hopping matrix element. Transport in the gold terminals in the substrate of Fig. 1 is modeled using single-channel ideal leads. Since gold is an *s*-orbital metal, only its $6s$ orbital is considered and this is assigned a site energy of -10 eV (the equilibrium Fermi energy for this model). The hopping energy of the gold leads was taken to be -3.5 eV. The sulfur atoms are modeled using their $3p$ orbitals, which have a site energy of -11 eV. To simulat charge transfer, a single gold atom is bonded beneath each sulfur atom. (If the sulfur atoms were coupled directly to the ideal leads, the surface charging that occurs at the interface between the sulfur atoms and the gold surface would be neglected. These single gold atoms are used to simulate the physics of the surface layer of gold and the chemistry of the sulfur atoms binding over hollow sites on the gold surface.) Each of these gold atoms is coupled to a single-channel lead. They are positioned 2 Å above the equipotential surface (depicted in Fig. 8 of the Appendix). Thus the equipotential surface is assumed to begin below the surface layer of the gold leads. To simulate the strong binding that occurs when sulfur binds over a hollow site on the gold surface, each of these gold atoms is strongly bonded to its sulfur atom and this is quantified by a hopping energy of -2 eV. Each sulfur is assumed to be positioned 2 Å above its gold atom. Similarly, the binding between the sulfur atoms and the carbon is assumed to be strong, and this hopping energy is assigned a value of -2 eV. The sulfur-carbon bond is taken to be 1.8 Å. The fractional charging energy U that multiplies the linear term in q in the site energy for each of these orbitals was taken to be 11.5 eV for the C $2p$, 9.7 eV for the S $3p$, and 8.6 eV for the Au $6s$ orbitals.[20]

The above methods together with the results of the Appendix for the electrostatic potential due to the metal terminals were used to calculate the current as a function of gate voltage through a MWT based on the $C_{13}S_4H_{11}$ molecule. (This is similar to the molecule depicted in Fig. 1 but has two more CH groups.) A symmetric source-drain bias voltage of 1 V was assumed and gate voltages up to a bias of -5 V (i.e., $+5$ eV for an electron) were studied. We found that charge is transferred to the chain. This is consistent with the polymer literature which reports charge transfer from the metal to carbon chains. However, it was also found that the electric current along the carbon chain was resistant to the application of the gate voltage. Electron transport along the backbone remained unhindered, and the current was almost independent of the gate bias voltage (the circles in Fig. 2). This indicates that in a functioning MWT the gate needs to interact with the chain molecule much more strongly than it does in the system considered above.

Our proposed solution to this problem is to adsorb onto the surface of the gate an atomic species that charges up as the gate voltage is applied and thus enhances the effective electrostatic interaction between the gate and chain molecule. We have chosen sulfur since it binds readily to gold surfaces and gains charge from the gold surface of the gate as a bias is applied to the gate in this model. (For the narrow nanoscale gates considered here, there is a substantial electric field in the vicinity of the gate due to the applied gate bias which helps to push charge onto the adsorbed sulfur atom. For much wider gates this effect is lessened significantly as the surface electric field is much weaker.) For the same chain molecule as above, a single sulfur atom adsorbed on the gate was modeled by situating it 2.5 Å below the middle carbon atom of the chain. Again this sulfur atom was bonded over a single gold atom so as to simulate the charge transfer that would take place in the physical system. The

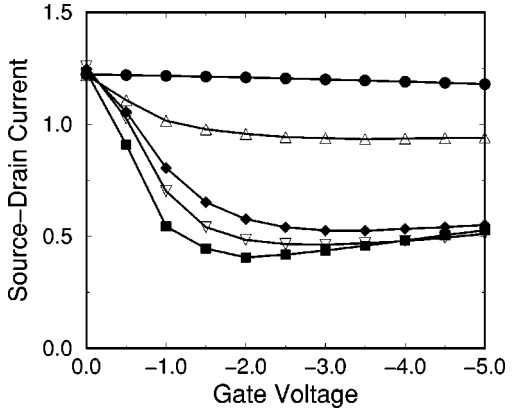

FIG. 2. The current as a function of gate bias voltage. The source-drain bias is 1 V. Circles: $C_{13}S_4H_{11}$ with no S atoms on the gate. Up triangles: $C_{13}S_4H_{11}$ with one S on the gate. Diamonds: $C_{15}S_4H_{13}$ with two S on the gate. Down triangles: $C_{17}S_4H_{15}$ with three S on the gate. Squares: $C_{19}S_4H_{17}$ with four S on the gate. The units of current are $(2e/h)$ eV.

gold atom was then attached to a single-channel ideal lead. Now, as the gate voltage is applied, the sulfur charges up, and this extra local charge results in an electrostatic potential barrier that can significantly reduce the current flowing through the molecular wire. (Note that this sulfur atom should not bond to the π carbon backbone since its p orbital is orthogonal to it.[21] Although it may modify the σ-bonding structure, it should also not form any σ bonds since these are saturated along the carbon chain.) The results are shown in Fig. 2 (up triangles) for a 1 V source-drain bias. There is now a clear reduction in the current as the gate voltage is increased.

A MWT with a second sulfur atom also adsorbed on the gate is depicted in Fig. 1. [The sulfur atoms on the gate are 2.8 Å apart—this corresponds roughly to the distance between hollow sites on an ideal (100) gold surface.] The two sulfur atoms together have a stronger effect on the current. This is shown in Fig. 2 (diamonds); the current is now reduced by a factor of 3 at a gate voltage of -2.5 V. This significant reduction in the current is due to the formation of a large potential energy barrier along the wire.

The self-consistently calculated site energy of each atom is plotted in Fig. 3. First the 0 V gate voltage result [Fig. 3(a)] should be noted. The source is held at -0.5 V ($+0.5$ eV electron energy) and the drain at $+0.5$ V. Right at the interface between the gold and the thiol, a potential barrier is formed due to charge transfer. (Including the single gold atoms between the ideal leads, which are assumed to form an equipotential, and the sulfur allows this barrier to be modeled in the present calculations.) The potential along the carbon chain is roughly flat due to charge rearrangement on the chain. Figure 3(b) shows the site energy along the wire at a gate voltage of -3 V. There is now a significant electrostatic potential barrier in the middle of the carbon chain. The potential barrier is not smooth, but consists of peaks and valleys due to alternating distances between the carbon atoms and the adsorbed sulfur atoms on the gate in Fig. 1.

This barrier hinders electron transport as is seen in the plot (Fig. 4) of the transmission probability of an electron from the source to the drain. The reduction in transmission

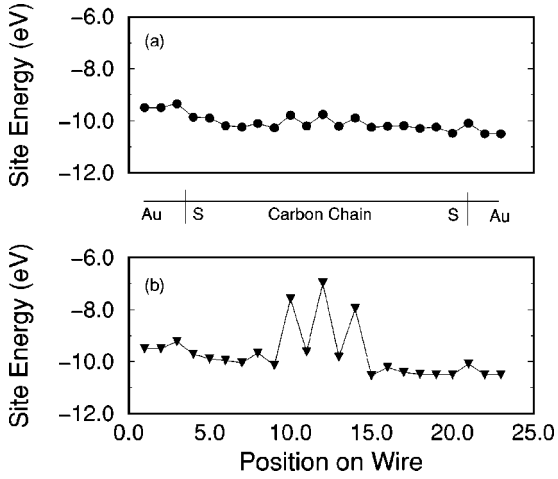

FIG. 3. This figure depicts the site energy of each atom along the chain. For each graph, the source-drain bias voltage was 1 V. (a) Graph for gate bias of 0 V and (b) graph for gate bias of -3 V.

probability is associated with the formation of a gap in the sequence of resonant states around the Fermi energy, as can be clearly seen in Fig. 4. At zero gate voltage [Fig. 4(a)] there is a strong resonance at the Fermi energy of -10 eV. Figure 4(b) corresponds to a gate voltage of -3 V and there is now a clear gap between the resonant states around the Fermi energy. For longer carbon chains with more sulfur atoms on the gate the nearly periodic structure of the barrier creates the equivalent of a band gap with the Fermi energy lying near the edge of the lower energy band. The molecule transmits electrons quite well at energies outside the band gap that forms around the Fermi energy. Increasing the length of the barrier suppresses transmission further in the band gap. However, because the Fermi energy lies near the edge of the bottom transmitting band, as the gate voltage is increased further, eventually the resonant states in the lower band begin to transmit a net current and the current rises. Stronger transistor action could be achieved for a Fermi energy more centered within the gap. However, in the simulations, charge transfer has the effect of keeping the lower lying resonances fairly close to the Fermi energy. Up to four sulfur atoms on the gate were simulated, thus increasing the length of the barrier and further reducing the current as shown in Fig. 2. For these longer chains the cur-

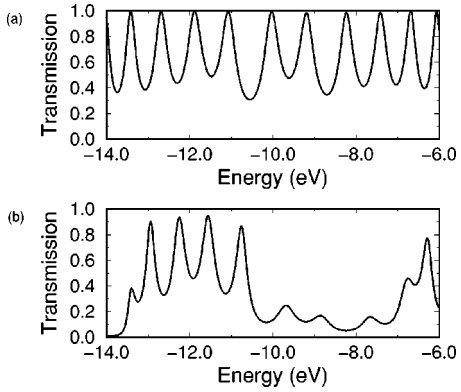

FIG. 4. Transmission probability for an electron to scatter through the chain. (a) corresponds to a gate bias of 0 V and (b) has a gate bias of -5 V. The source and drain are biased at 1 V.

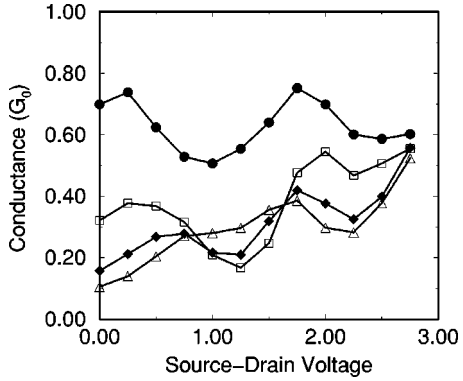

FIG. 5. Differential conductance of molecular wire as a function of gate bias and source-drain bias: (filled circles) zero gate bias, (open squares) 1 V gate bias, (filled diamonds) 2 V gate bias, (open triangles) 3 V gate bias. The units are in $G_0 = 2e^2/h$.

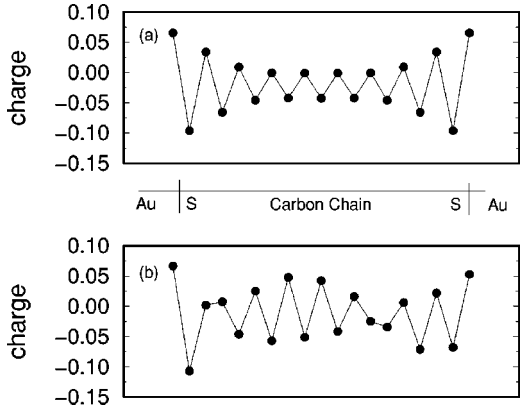

FIG. 6. Fractional charge along the wire at zero gate bias. (a) Results for a source-drain bias of 0 V. (b) Results for a source-drain bias of 1 V.

rent rises at higher gate voltages, as expected from the above arguments.

To gain further insight into the transport properties of these chains, the differential conductance of the molecular wire with two sulfur atoms adsorbed on the gate is plotted at various gate voltages as a function of source-drain bias in Fig. 5. The figure shows at which source-drain bias and at which gate voltage optimal transistor action can be achieved. The top curve with filled circles corresponds to zero gate bias. The peaks in the conductance correspond to resonant transmission through the resonances near the Fermi energy. The other graphs correspond to different reverse biases applied to the gate. For low source-drain voltages, the conductance of the molecule is clearly lowered due to the barrier being formed. However, because the Fermi energy of the leads resides near the edge of the lower band of resonant states as was discussed above, for sufficiently high source-drain biases the molecule can be made to conduct appreciably even when a large reverse bias is applied to the gate. Optimal transistor action can be achieved by operating in a regime where there are clearly high and low conducting states. This can be achieved at source-drain biases near 0 V by varying the gate bias from 0 V to -3 V. Here the conductance varies from approximately $0.7G_0$ to $0.1G_0$. Other favorable operating voltages correspond to a source-drain bias around 1 V and a gate bias between -1 and -2 V. Here the conductance varies between $0.5G_0$ and $0.2G_0$.

Examination of the calculated fractional charge along the molecular chain also reveals some interesting phenomena. The results that follow are for the molecular wire with two sulfur atoms adsorbed on the gate. As mentioned above, undimerized chains were assumed in the calculation. Figure 6 shows results for the charge along the wire at zero gate bias. The plot in (a) corresponds a zero source-drain bias. The first thing to be noted is the charging at the contacts between the gold and the sulfur atoms. The gold loses charge, and the sulfur acquires charge, which leads to the formation of the Schottky-like barrier seen in the previous plots of the potential. Along the carbon chain a commensurate charge density wave with a period of two atomic spacings is formed. Particularly interesting are the corresponding results shown in (b) for the charge along the chain when a 1 V source-drain bias is applied: The phases of the charge density wave at the two ends of the carbon chain are pinned by the chemical charge transfer that occurs there between the gold and sulfur atoms. Thus when the applied source-drain bias breaks the left-right symmetry along the chain, the charge redistribution along the chain proceeds through the formation of a soliton-antisoliton pair along the wire; the net charge of the soliton near the right end of the wire is negative and of that on the left is positive as one might expect intuitively based on the sign of the source-drain bias. Notice also the associated π shifts in the phase of the charge density wave across the soliton and across the antisoliton—this is most easily seen by comparison with the phase of the charge density wave at zero source-drain bias shown in Fig. 6(a).

To gain further insight into the role of the solitons in this system, consider the charge modulation along the wire at a gate voltage of -3 V that is plotted in Fig. 7. In (a) the results for a zero source-drain bias are shown. In this case the phase of the charge density wave at the ends of the chain is pinned by the chemical charge transfer as before, but over the gate electrode it is pinned in *antiphase* with the zero gate voltage case [shown in Fig. 6(a)] by the interaction with the charged sulfur atoms on the gate. Because of this there are two symmetric solitons near the ends of the wire in Fig. 7(a). In contrast to the case shown in Fig. 6(b), here *both* solitons carry a net negative charge which is a manifestation of the

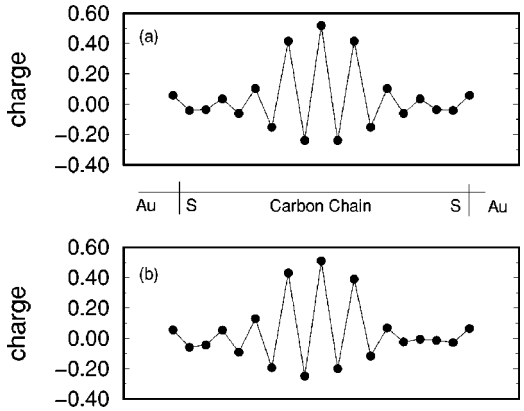

FIG. 7. Fractional charge along the wire at -3 V gate bias. (a) Results for a source-drain bias of 0 V. (b) Results for a source-drain bias of 1 V.

symmetric redistribution of the electronic charge density from the center of the wire toward its ends in response to the negative bias voltage applied to the gate.

When a 1 V source-drain bias is applied to this system [Fig. 7(b)] another soliton appears to be forming near the right end of the wire between the last two carbon atoms, again breaking the left-right symmetry of the charge distribution in response to the applied source-drain voltage. Thus the system responds to the application of moderate gate or source-drain voltages through the formation of additional solitons along the wire.

Further investigation of the dynamics and energetics of the formation of solitons in these carbon chains and of the underlying physical mechanisms will clearly be of interest.

VI. CONCLUSIONS

In summary, we have provided a theoretical framework for modeling current flow and charging effects in multiterminal molecular wire systems. Included in our methodology is a procedure for evaluating the self-consistent electrostatic potential in the region of the molecule due to application of voltages on the different terminals. It is based on an extension of tight-binding theory to allow for fractional charging. Also taken into consideration is the induced charge on the metallic leads, which is handled by means of image charge potentials.

This theory was applied to the simulation of a molecular wire transistor that can be realized using presently available experimental techniques. It was shown that it is feasible to control the current flowing through this device by the application of a gate voltage. The key to controlling the current is the use of a suitable adsorbate on the gate electrode that is effective in mediating the gate voltage onto the molecular wire. It was also shown that charged solitons form along the wire in response to the application of voltages to the terminals. Further research into the dynamics of these solitons will be of interest. The incorporation of a third terminal into molecular wire systems as described in this work should open up many exciting possibilities in the science and technology of molecular nano-electronic devices.

ACKNOWLEDGMENTS

We thank R. Hill, M. A. Reed, H. Guo, B. Heinrich, M. Freeman, J. Young, and M. Moskovits for rewarding discussions. This work was supported by NSERC and by the Canadian Institute for Advanced Research.

APPENDIX: POTENTIAL FOR THREE-TERMINAL GEOMETRY

This Appendix evaluates the electrostatic potential associated with the terminals and image charges that is used in the simulation presented in Sec. V. The geometry that is considered here is a planar three-terminal configuration (this is shown in Fig. 8). It consists of a substrate divided into three regions. The first region from $-3L/2<x<-L/2$ acts as the source, the second region from $-L/2<x<L/2$ acts as the gate, and the third region from $L/2<x<3L/2$ is the drain. (In reality such a substrate would have insulating dielectrics between the three regions, but that is not considered explicitly here.) The distance perpendicular to the substrate is measured by the coordinate z. The potential $\phi(\vec{r})$ satisfies Laplace's equation[22]

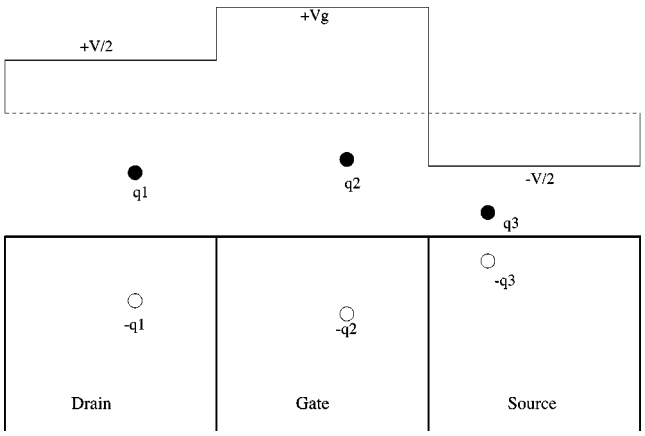

FIG. 8. A schematic of the three-terminal electrostatic problem. The metallic substrate is divided into three equal sized regions that act as the source, the gate, and the drain. The source is held at constant potential of $-V/2$, the gate at V_g, and the drain at $V/2$. A charge q above the metallic conducting substrate generates an image charge at an equal distance below the surface of the conductor.

$$\frac{\partial^2\Phi(x,z)}{\partial z^2}+\frac{\partial^2\Phi(x,z)}{\partial x^2}=0 \tag{A1}$$

subject to the boundary conditions $\phi(x,0)=-V/2$ for $-3L/2<x<-L/2$, $\phi(x,0)=V_g$ for $-L/2<x<L/2$, and $\phi(x,0)=V/2$ for $L/2<x<3L/2$.

The above equation has the solution

$$\Phi(x,z)=\int_{-\infty}^{\infty} d\alpha\, e^{i\alpha x}e^{-\alpha z}c(\alpha). \tag{A2}$$

Applying the boundary condition at $z=0$ gives

$$\Phi(x,0)=\int_{-\infty}^{\infty} d\alpha\, e^{i\alpha x}c(\alpha). \tag{A3}$$

Performing the inverse transform allows the solution for $c(\alpha)$,

$$c(\alpha)=\frac{1}{2\pi}\int_{-\infty}^{\infty} dx\,\Phi(x,0)e^{-i\alpha x}. \tag{A4}$$

With the boundary conditions above, it is found that this gives

$$c(\alpha)=\frac{1}{2\pi}\left\{\frac{V}{i\alpha}\left[\cos\left(\frac{3L\alpha}{2}\right)-\cos\left(\frac{L\alpha}{2}\right)\right]+\frac{2V_g}{\alpha}\sin\left(\frac{L\alpha}{2}\right)\right\}. \tag{A5}$$

Inserting this back into Eq. (A2) and integrating gives the following expression for the potential:

$$\Phi(x,z)=\frac{1}{2\pi}\left\{-V\left[\arctan\left(\frac{3L/2+x}{z}\right)-\arctan\left(\frac{3L/2-x}{z}\right)+\arctan\left(\frac{L/2-x}{z}\right)-\arctan(L/2+xz)\right]+2V_g\left[\arctan\left(\frac{L/2+x}{z}\right)-\arctan\left(\frac{x-L/2}{z}\ t\right)\right]\right\}. \tag{A6}$$

The last problem that remains is to find the image potential arising from the presence of charge $\{q_j\}$ on the molecule. The substrate is assumed to form a perfect planar conductor, and hence the method of images applies. For a charge q_j at $\vec{r}_j=(x_j,y_j,z_j)$, there is mirror image charge $-q_j$ at $(x_j,-y_j,z_j)$. Thus the image potential at position $\vec{r}=(x,y,z)$ is

$$(\phi_{image}(\vec{r},\vec{r}_j))_j=\frac{-q_j}{4\pi\epsilon_0}\frac{1}{\sqrt{(x-x_j)^2+(y+y_j)^2+(z-z_j)^2}}. \tag{A7}$$

The total image potential is found by summing over image potentials arising from all the charges $\{q_j\}$ on the molecule.

[1] R.P. Andres, J.D. Bielefeld, J.I. Henderson, D.B. Janes, V.R. Kolagunta, C.P. Kubiak, W.J. Mahoney, and R.G. Osifchin, Science **273**, 1690 (1996).

[2] L.A. Bumm, J.J. Arnold, M.T. Cygan, T.D. Dunbar, T.P. Burgin, L. Jones II, D.L. Allara, J.M. Tour, and P.S. Weiss, Science **271**, 1705 (1996).

[3] M.A. Reed, C. Zhou, C.J. Muller, T.P. Burgin, and J.M. Tour, Science **278**, 252 (1997).

[4] J. Chen, M.A. Reed, A.M. Rawlett, and J.M. Tour, Science **286**, 1550 (1999).

[5] J.K. Gimzewski and C. Joachim, Science **283**, 1683 (1999).

[6] B.C. Stipe, M.A. Rezaei, and W. Ho, Science **280**, 1732 (1998).

[7] C. Joachim and J.K. Gimzewski, Chem. Phys. Lett. **265**, 353 (1997).

[8] S. Datta, W. Tian, S. Hong, R. Reifenberger, J.I. Henderson, and C.P. Kubiak, Phys. Rev. Lett. **79**, 2530 (1997).

[9] S.N. Yaliraki, M. Kemp, and M.A. Ratner, J. Am. Chem. Soc. **121**, 3428 (1999).

[10] N.D. Lang and Ph. Avouris, Phys. Rev. Lett. **84**, 358 (2000).

[11] M. Di Ventra, S.T. Pantelides, and N.D. Lang, Phys. Rev. Lett. **84**, 979 (2000).

[12] E. Emberly and G. Kirczenow, Phys. Rev. B **58**, 10 911 (1998).

[13] R. Landauer, IBM J. Res. Dev. **1**, 223 (1957); Phys. Lett. **85A**, 91 (1981).

[14] M. Büttiker, Phys. Rev. Lett. **57**, 1761 (1986).

[15] T. Christen and M. Büttiker, Europhys. Lett. **35**, 523 (1996).

[16] E. Emberly and G. Kirczenow (unpublished).

[17] S. P. McGlynn, L. G. Vanquickenborne, M. Kinoshita and D. G. Carrol, *Introduction to Applied Quantum Chemistry* (Holt, Rinehart and Winston, Inc. New York, 1972), Chap 3.

[18] S.J. Tans, M.H. Devoret, and C. Dekker, Nature (London) **386**, 474 (1997).

[19] S.J. Tans, R.M. Veschueren, and C. Dekker, Nature (London) **393**, 49 (1998).

[20] S. Alvarez (unpublished). For Au, see S. Komiya, T.A. Albright, R. Hoffmann, and J.K. Kochi, J. Am. Chem. Soc. **99**, 8440 (1977). For C and H, see R. Hoffmann, J. Chem. Phys. **39**, 1397 (1963). For S, see M.M.L. Chen and R. Hoffmann, J. Am. Chem. Soc. **98**, 1647 (1976). For the self-consistent charge parameters of C and S see Ref. 17; and for Au a least-squares fit to the data of O.P. Charkin' [Russ. J. Inorg. Chem. **19**, 1589 (1974)] was used.

[21] H. Sellers, A. Ulman, Y. Schnidman, and J.E. Eilers, J. Am. Chem. Soc. **115**, 9389 (1993).

[22] J.D. Jackson, *Classical Electrodynamics* (John Wiley and Sons, Inc., New York, 1975).